BEE 453

Computer Aided Engineering:

Applications to Biomedical Engineering

Lord of the Mood Rings

Final Project

May 5, 2003

Celia Chan
Yen Cu
Jessica Kadlec
Jennifer Lee

Table of Contents

1.0 Executive Summary

Our main objective is to study the mechanisms by which heat transfer taking place in the human finger will affect the color change in the mood ring. This project uses GAMBIT and FIDAP to model the heat transfer from the finger to the ring. Finding the possible range of heat generations, one can estimate the temperature range of the surface and thus the best type of LC to be used in a ring. By determining the temperature in the ring at steady state the blood flow rate can be quantified, which will provide the required heat generation to change the mood ring to any desired color. We obtained several Q's ranging from 6800 to 7200 W/m^3 appropriate to blood flow rate, and ambient conditions with no forced convection for the model. Further sensitivity analysis was done for selected data input, such as conductivity and source term, to assess their impact on the results. It was concluded that blood flow rate corresponding to the heat generation values used ranged from 0.245 to 0.265 cm^3/min. From the results it is recommended that the color change in the LCD crystal should be most sensitive over the range of 32 to 35 °C.

2.0 Introduction

Since their first production in the 1970s, mood rings continue to be popular among trendy consumers today. They are a cheap and accessible "predictor" of a person's mental state. Commercially, the wearer of a mood ring that turns blue is considered to be "relaxed", while one whose ring stays black could be "anxious" or "stressed". However, the color change is dependent on more than the seemingly metaphysical effect of moods. The mood rings have glass-enclosed thermotropic liquid crystals. These liquid crystal molecules are very sensitive; they change position, or twist, according to changes in temperature. This change in molecular structure affects the wavelengths of light that are absorbed or reflected by the liquid crystals, resulting in an apparent change in the color of the stone.

Major factors such as the ambient temperature, wind conditions, and heat generation in the finger affect the color of the liquid crystal. At constant ambient temperature and wind condition, the varying heat generation of the finger is the sole cause of color change. This heat generation results from arterial blood flowing through the finger, which carries higher body core temperature. Depending on the wearer's physical condition, more often triggered by mental states, the blood flow rate through the finger will vary. An increased blood flow results in elevated heat generation for the finger.

Arrays of liquid crystals (LC), with wavelength output dependent on varying range of temperature, are manufactured for different uses. Some examples of the temperature ranges that an LC may respond are 25^{o}C - 30^{o}C, 29^{o}C - 35^{o}C, 34^{o}C - 40^{o}C, or 35C-41C. With such overlap in ranges, precise temperature range is impertinent to provide the most efficient use of the diverse color output. Our analysis aim to find an LC that will produce a desirable color based on given blood flow rate, thus enable the wearer to "customize their moods".

3.0 Design Objective

In this report, we study the mechanisms by which heat transfer takes place in human fingers to produce the changing colors. The temperatures at which these color changes occur are of interest. The composition of the finger (epidermis, muscle and blood flow) affects the rate at which heat can travel radially through the finger to be released to the surrounding environment. The possible range of heat generations by the finger will demonstrate the best type of liquid crystal to be used in a ring to provide the wearer of the ring the pleasure of experiencing change in the color that corresponds to the change in finger temperature.

We propose to apply different blood flow rates, thus different heat generation in human fingers and therefore find a range of heat transfers for which a typical mood ring must be effective. Our calculations will be made using a constant metal thickness of 1.0 mm for each ring. The schematic for mesh generation will be the axial symmetric model of the finger, compose of the ring layer, epidermis, muscle/fat and the bone layer. We will try to determine the rate at which heat generated by the body at the base of the finger corresponding to a certain flow rate using the Bioheat equation. The temperature conducted through the metal and liquid crystal will be calculated for a fixed ambient condition. The final solution of the problem will be at steady state with ambient temperature at 25^{o}C with no convection. We will use a mesh simulation and compare the different rates of heat transfer for different blood flow rates.

4.0 Schematic

Schematic 1: Schematic of human finger and ring.

The finger is composed of bone, muscle, fat, and skin layers with more muscle and fat lying in the palm side. To simplify the geometry, the layers were assumed to be symmetrical around the bone with constant width through the length of the finger. With these simplifications, it was possible to come up with rectangular area for each of the finger layers and axis symmetrical around the center, such as in Schematic 1.

5.0 Results

Many simplifying assumptions were used in the design of our model:

- The finger is assumed to be symmetric around the center axis.
- Each tissue layer has constant properties.
- Most of all heat generation is coming from the flesh layer that consist of muscle and fat, thus heat generation in other parts of the finger, such as the bone, is negligible.
- The finger has an infinite geometry in z-direction with radial heat flow outward; thus assuming that the endings are insulated.
- Blood flow is laminar and incompressible
- Ambient temperature and humidity remains constant

The metabolic heat generation from the blood flow varies greatly throughout the body. Blood flow rates are higher in major blood vessels closer to the heart than the smaller blood vessels and capillaries in the fingers and toes; on average finger temperature is 33°C. We were able to determine which heat generation value correspond to blood flow rate in the finger using the bioheat equation (Table 2,3,4 in Appendix). The bioheat equation allows one to calculate the volumetric blood flow per unit volume of tissue. Multiplying this by the tissue volume yields the blood flow into the finger. Our original solution consists of only the flesh as a heat source ($Q = 7000 W/m^3$). This heat source term included both the heat generation that comes from blood flow and the metabolic heat generation coming from the cells, which is 1800 W/m^3.[8]

Figure 1 shows the mesh generated for our analysis. Even though the finger constantly generates heat, the ring remains cold relative to the finger. The ring acts as a heat sink because of the high conductivity of the metal.

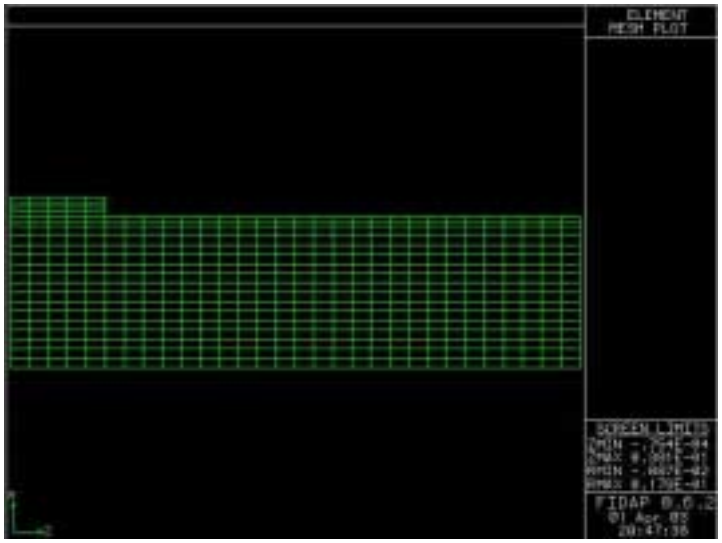

Figure 1: Mesh Plot of the Axis Symmetric Finger

Given the heat generation, Q = 7000 W/m^3 with ambient conditions h_c = 0.5W/m^2 and $T_{ambient}$ = 25^{o}C, the temperature within the finger vary from 33.2 ^{o}C - 33.62^{o}C (Figure 2). The temperature is lowest in the region around the ring, and highest for the region near the axis and away from the ring. Temperature profile is plotted for the distance from the center of the bone (axis) to the middle of the ring surface (Figure 3). The distance vs. temperature plot shows that the temperature is variable throughout the flesh region (x = -.0035 to 0 m), but becomes almost constant in the ring. The region of interest is x = 0.0005 to 0.0015, which corresponds to the region of the ring. The high conductivity and the tiny thickness of the metal produce an almost constant temperature profile of 33.2^{o}C throughout the ring.

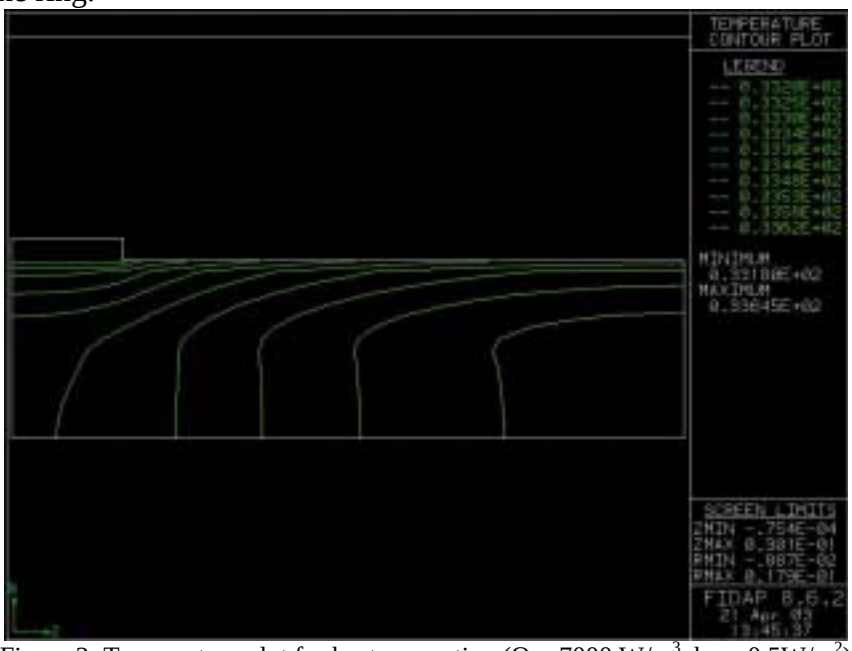

Figure 2: Temperature plot for heat generation (Q = 7000 W/m^3, hc = 0.5W/m^2)

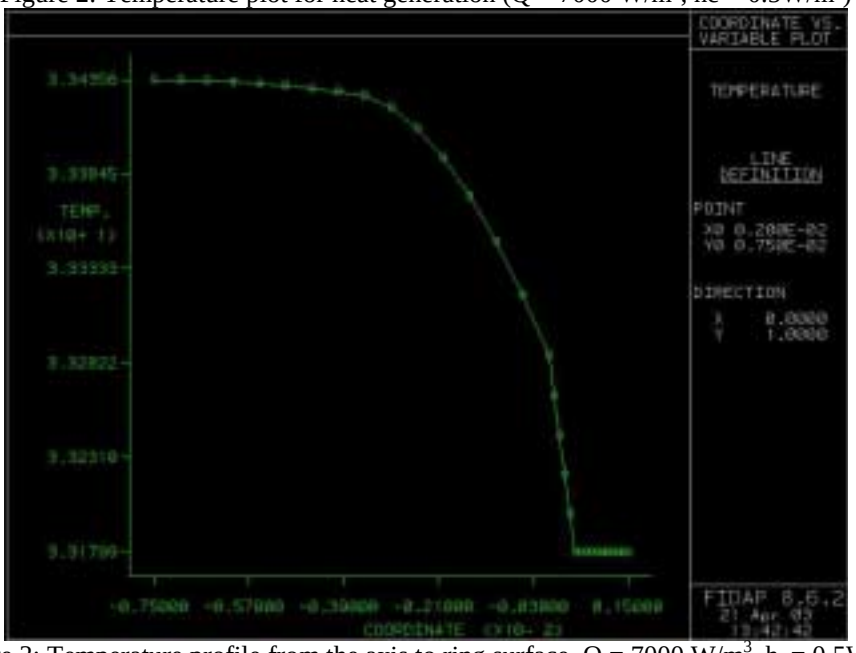

Figure 3: Temperature profile from the axis to ring surface. Q = 7000 W/m^3, h_c = 0.5W/m^2

The minimum temperature calculated by FIDAP occurred in the ring itself, while the maximum value was found in the bone. The minimum and maximum values corresponding to a range of heat generation values can be viewed in Graph 1. There is a linear relationship between the heat generation and the temperature, and as seen in the graph the difference in temperature between the minimum and the maximum value remains constant over the heat generation values tested.

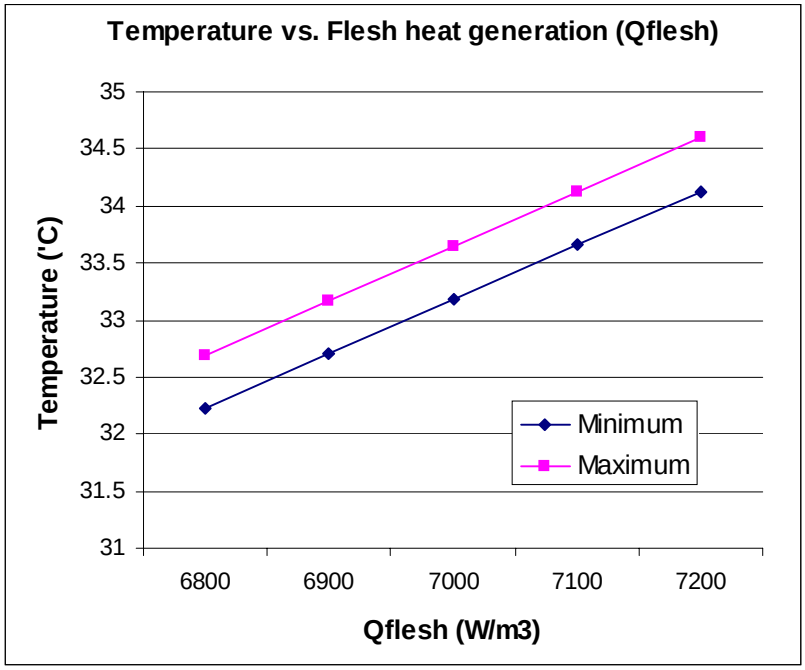

Graph 1: Temperature profile of flesh heat generation

The temperature profile was reasonable for our model. The ring acted as a heat sink and thus the skin temperature near the ring was less than that toward the far end of the finger (Figure 2). The high conductivity in the ring resulted in an almost uniform temperature across the ring, as opposed to the gradient observed in the finger (Figure 3). The blood flow rate was found to be on the order of $0.25cm^3$/min. The blood flow values varied slightly with a large change in heat generation values, as seen in Table 3 (Appendix C). This leads us to conclude that the heat generation is highly dependent on the blood flow rate. The blood flow rate finger is much slower than the blood flow rate of the vessels closer to the heart because vessels in the finger are mainly capillaries with very tiny cross-sectional area and flow rate decreases as blood moves away from the heart. Considering the small volume of the finger relative to the total mass of the human body and its extremity from the heart, the blood flow rate used for the finger is much smaller than the arterial blood flow.

6.0 Sensitivity Analysis

Sensitivity analysis is used to ascertain how a given model output depends upon the input parameters. By conducting a sensitivity analysis, we can ensure both accuracy and precision of results. Our sensitivity analysis involves the alteration of the number of nodes in the mesh, the node shape, source term(s) Q, heat coefficient and conductivity of skin and

ring. We refined our mesh in order to test for convergence. Appendix B, 8.2.6 shows two refined meshes, one which is a triangular mesh with nodes concentrated near the ring and the second which consists of evenly distributed rectangular mesh. The contour lines produced by the finer rectangular mesh are smoother than that of the triangular mesh but are the same general lines. Thus the remesh shows convergence of the solution.

6.1 Source Term

Blood transported in and out of the finger layers is the main source of heat. Our original solution consists of only the flesh as a heat source ($Q = 7000W/m^3$). However it is known that blood vessels are also embedded inside the bone because oxygen and other compounds are needed inside the bone as well. Thus for sensitivity analysis, we included heat generation in the bone as well as the flesh. The heat source terms tested for bone and flesh were both lower than the previous approximation of 7000 W/m^3, due to the fact that the greater volume with the same volumetric heat generation resulted in temperatures higher than normal body temperature (Appendix A, 8.1.5 Table 4).

6.2 Conductivity (k)

Our model assumes radial heat transfer solely by conduction. Thus conductivity is an important factor in determining temperature. We conducted sensitivity analysis on k_{skin}, with the original value of 0.1W/mK, by running the solution for a 10% decrement of this value (0.09W/mK)

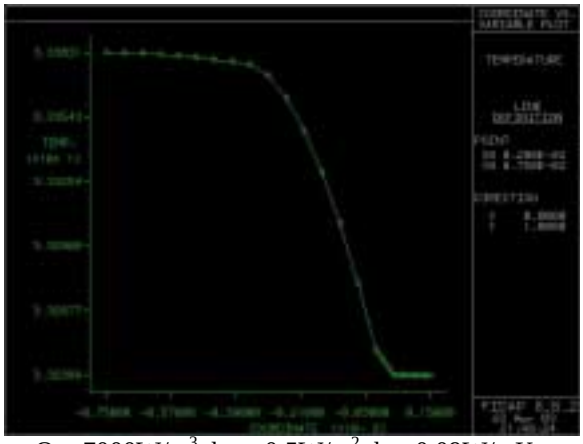

$Q = 7000W/m^3$, $hc = 0.5W/m^2$, $k = 0.09W/mK$

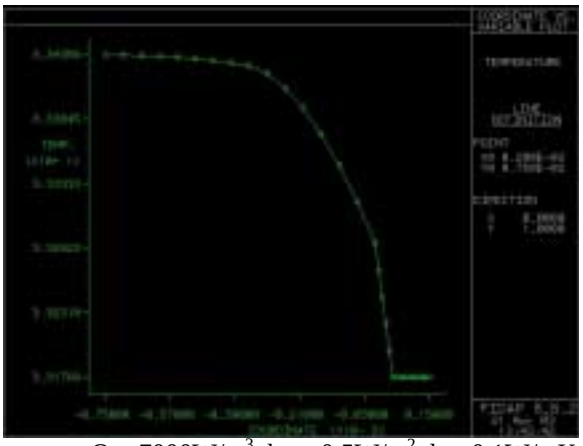

$Q = 7000W/m^3$, $hc = 0.5W/m^2$, $k = 0.1W/mK$

As shown, the conductivity of the skin ($x = -0.02 – 0.5$) has a significant effect on the temperature profile. However the final temperature in the ring has changed from 33.18^oC to 33.24^oC from the original (increase of 0.2%). Because our main interest is the temperature of the ring at steady state, the change in the temperature profile is inconsequential. To further see the effect of change in conductivity of the ring, a temperature profile for $k_{ring} = 1W/mK$ were obtained.

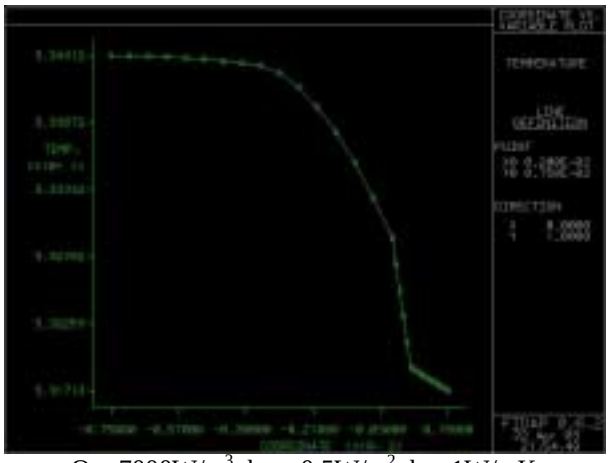

Q = 7000W/m^3, hc = 0.5W/m^2, k = 1W/mK

The reduction of 2 magnitudes from original value 429 W/mK produced the conductivity value of k_{ring} = 1W/mK. This time, the contour line varies for x in the location of the ring. Yet the resulting temperature for the ring approximates 33.17^{o}C with only a 0.03% change. Thus we can say that the conductivity of the ring does not have any significant impact on the result, perhaps due to the fact that the ring is quite thin (1mm). Therefore we further conclude that the type of material used to make the ring does not significantly impact the resulting LC temperature at steady state.

To determine the influence of our schematic to the solution, we added a layer of fat (0.3mm) beneath the skin. For Q_{flesh} = 7000W/m^3, the average skin temperature came to be 50^{o}C; this is due to the insulating effect of the fat layer. Also, the higher temperature results because we took the conductivity of the flesh to still be a combination of muscle and fat. However, the temperature profile across the finger and the difference in maximum and minimum temperature is similar to the original schematic without the fat layer (Appendix C, 8.3, Sensitivity analysis plot: Fat layer).

7.0 Conclusion, Design Recommendation and Difficulties

Blood flow into finger is the major source of heat generation and the steady state temperature. Even a small change in blood flow can induce a significant temperature change in the skin surface. In ambient temperature of 25ºC, surface temperature in the finger ranges from 32.232ºC to 34.128ºC and the blood flow through the finger is from 0.245-0.265cc/min

Our study did not include the different layers of the ring. The glass covering for the LC might change the amount of heat escaping due to convection. Therefore, including a glass layer between the metal ring and the surrounding will produce more accurate temperature values. In addition, a 3-D mesh rather than 2-D will create more precise depiction of the varying sizes of muscle, fat, and skin layers. For more accurate results, we recommend separating the muscle and fat layers in the flesh.

Many factors are involved in the cost of the mood ring. The target consumer for this product is mostly teenagers, who have very limited assets; thus the price of the ring cannot be too expensive. The price of a ring can vary depending on the material used for the ring; the cost of the LC is negligible compared to the cost of the metal used to make the ring. For example, Edmund Industrial Optics sells LCs for mood rings for 22 dollars per sheet, which is fairly cheap. Among the various LCs that are produced, the product #72-373 is sensitive over our temperature range of 32 to 34 °C, and would be best for mood ring production (Appendix C). Silver and gold are good conductors of heat, but they are much more costly than sterling silver and plastic. The magnitude of conductivity in metals is so large compared to the conductivity of the biological materials, so the least expensive metal that can be used would result in the best and most cost effective design. The thickness could also have an effect on how fast the ring changes color, but again the conductivity of the metal is high enough that the surface temperature would probably not change significantly based on variable thickness alone.

Our project's main difficulty was in finding the various properties for the finger. Because we assumed a "reverse" approach, we found a heat generation value to get a reasonable range of blood flow rate in the finger. We were more interested, however, in the effect of blood flow rate on the heat generation, which induces the ring to change color. In this aspect, we found that there is a clear relationship between these variables. In the future, we propose to take a "forward" approach, where the heat generation is computed from the blood flow.

8.0 Appendices

8.1 Appendix A

8.1.1 Geometry

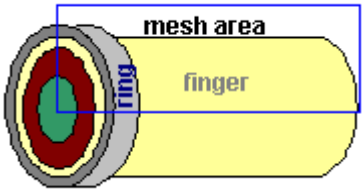

8.1.2 Governing equations

$$\rho_{tissue}\, C_{Ptissue}\, (\delta T/\delta t) = k[\delta^2 T/\delta z^2 + \delta/\delta r(r*\delta T/\delta r)] + Q$$

where $Q = \rho_{blood}\, C_{Pblood} V_{blood}\, (T - T_i)$, $\rho_{tissue}\, C_{Ptissue}\, (\delta T/\delta t) = 0$

final GE: $0 = k[\delta^2 T/\delta z^2 + \delta/\delta r(r*\delta T/\delta r)] + \rho_{blood}\, C_{Pblood} V_{blood}\, (T - T_i)$

- Q is metabolic heat generation.
- V_b is the volumetric rate of warm blood flow through the hand, of the dimensions [m^3_{blood}/m^3_{tissue}-s].
- The subscript "b" pertains to properties of the blood flowing through the hand.
- T_∞ and T refer to the ambient and solution temperatures at a node respectively.
- To model the phase change for tissue freezing, C_p refers to apparent specific heat values.
- We can refer to the product $\rho_b C_{pb} V_b$ as the "bioheat coefficient."

8.1.3 Initial Condition

Our study is based on steady state solution. Because of the high sensitivity of LC, time change is very miniscule. Our interest lies only on the final temperature on the surface of the ring.

8.1.4 Boundary Condition:

Ambient Temperature = 25 Degrees Celsius
Heat transfer coefficient = $0.5 W/m^2$
@ axis $\delta T/\delta r = 0$ (i.e. no heat flux through center)
@ left and right boundary of geometry $\delta T/\delta z = 0$ (ends are insulated)

8.1.5 Input Parameter

The properties for various tissue and silver were used as input in "Properties" in FIDAP.

Table 1: Tissue Properties[1]

Layer	Thickness (m)	Thermal Conductivity (W/mK)	Specific Heat (J/kG-K)	Density (kg/m^3)
Bone	8.00E-03	5.20E-01	1.26E+03	1.81E+03
Muscle/Fat	1.25E-03	3.20E-01	9.75E+02	3.10E+02
Epidermis	5.00E-04	1.00E-01	3.66E+03	1.10E+03
Silver[2]	5.00E-04	429	232	10490
Fat	0.001	0.21	800 [6]	290 [5]

Blood Property	Value	
Bioheat Coeff. (Muscle)	5.75E+02	Dimensionless
Specific Heat	3.89E+03	J/kg-K

Heat transfer coefficient for stationary air hc = 0.5w/m^2. [3]
(At velocity = 0m/s and reference temperature (included in hc input) is 25^oC)

To calculate the blood flow in the finger, we first found the tissue volume by using the dimensions from our schematic (Table 2). In Table 3, Q_{blood} was found by subtracting 1800W/m^3, the metabolic heat generation, from Q_{total}. Using $V = Q/\rho c(T-Ta)$, we found the blood flow per volume of tissue per second. Multiplying with the calculated tissue volume yields the blood flow rate in the finger (cc/min). As part of our sensitivity analysis, we also computed the blood flow when heat generation is in both the flesh and bone (Table 4).

Table 2: Volume of Tissues

Entity	Ri	ro	pi	L	volume (cm3)
bone	0	0.004	3.14159	0.08	4.0212352
flesh	0.004	0.0075	3.14159	0.08	10.1159198
Total					14.137155

Table 3. Heat generation (Q) in flesh

Q_{total} (W)	Q_{blood} (W)	V (cm^3 blood /cm^3 flesh*s)	Volume of tissue (cm^3)	Flow rate blood into tissue (cc/min)
6800	5000	4.042E-04	10.1159	0.2453
6900	5100	4.123E-04	10.1159	0.2502
7000	5200	4.204E-04	10.1159	0.2551
7100	5300	4.284E-04	10.1159	0.2600
7200	5400	4.365E-04	10.1159	0.2650

Table 4. Heat generation (Q) in flesh and bone

Q flesh, blood (W)	Q bone, blood (w)	V_{flesh} (cm^3blood/cm^3 flesh*s)	V_{bone} (cm^3blood/ cm^3 bone*s)	Volume flesh (cm^3)	Volume bone (cm^3)	Flow rate blood into tissue (cc/min)
3200	3200	2.587E-04	2.587E-04	10.1159	4.0212	0.2194
2200	2200	1.778E-04	1.778E-04	10.1159	4.0212	0.1509
4200	4200	3.395E-04	3.395E-04	10.1159	4.0212	0.2880
4200	2200	3.395E-04	1.778E-04	10.1159	4.0212	0.2490

8.2 Appendix B

8.2.1 Problem:

Geometry type	axi-symmetric
Flow regime	incompressible
Simulation type	Steady
flow type	Laminar
convective term	Linear

fluid type	Newtonian
Momentum eq	nomomentum
Temperature dependence	Energy
Surface type	Fixed
Structural solver	Nostructural
Elasticity remeshing	no remeshing
Number of phase	single phase

8.2.2 Solution:

Solution method	SS=10
Relaxation factor	ACCF=0

8.2.3 Time Integration:

Not applicable (steady state).

8.2.4 Boundary condition:

BC	flux
Flux type	heat

8.2.5 Region selection

entity:	bone mid flesh mid skin mid ring mid bone end flesh end skin end axis
Value generation:	constant =0

8.2.6 Convergence

The results should not be dependent upon the geometry of our system. In fact, when using a mesh to model a biological system with nodes and elements, we must make sure that the mesh is fine enough to provide convergent solutions. It has been shown that with very few nodes and elements, mesh provided very rigid and skewed solutions with inconsistent temperature distribution. With finer mesh, the temperature contour had very smooth curves.

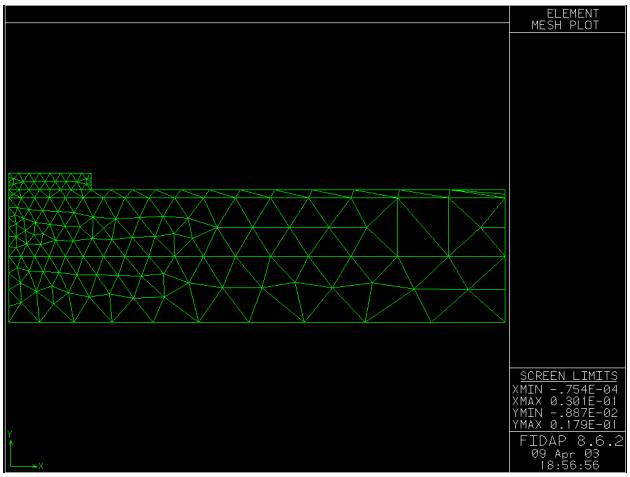

Remesh-1. Mesh using triangular nodes, with smaller nodes concentrated near the ring.

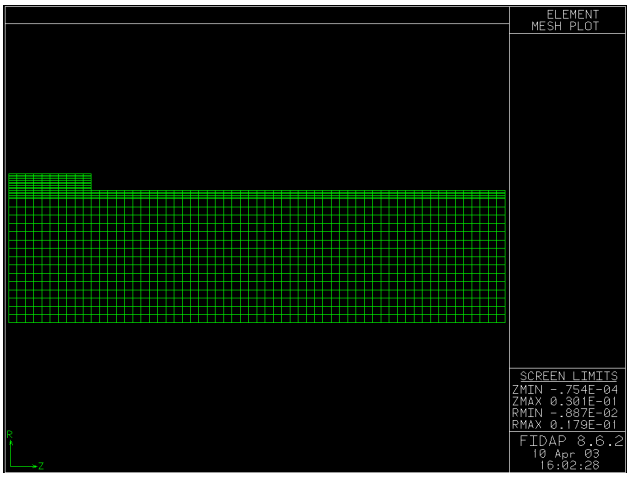

Remesh-2. Finer mesh with more rectangular nodes uniformly distributed over the geometry.

Remesh-1

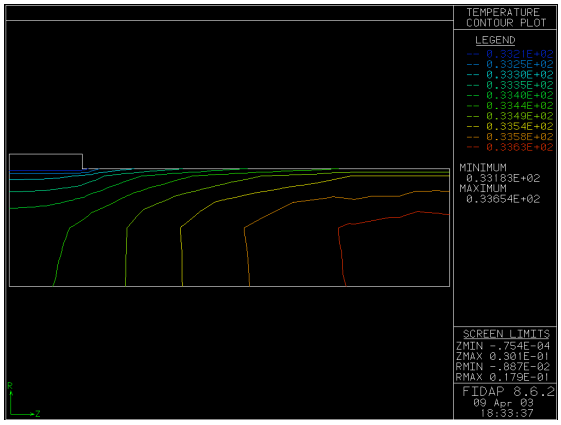

Remesh-2

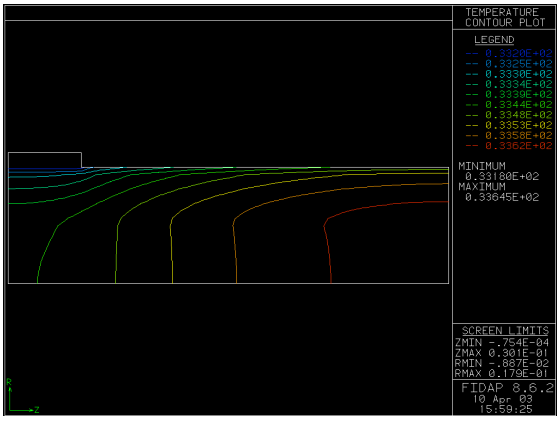

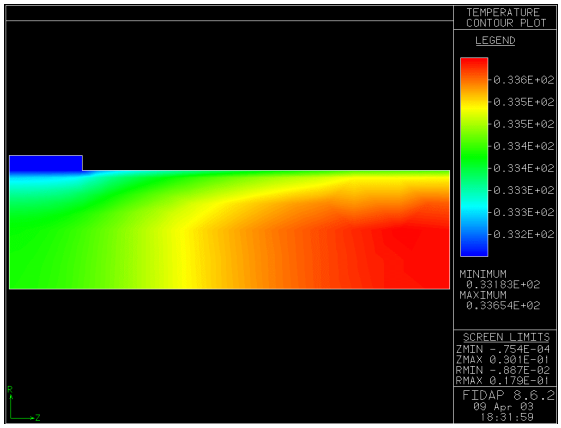

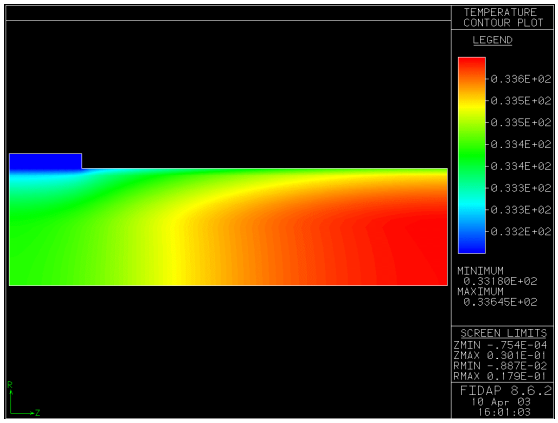

The mesh analysis shows that temperature contours are much smoother for remesh-2 (uniformly distributed rectangular nodes) especially at regions far from the ring. At the region near the ring, the contours are quite similar, but still smoother for remesh-2. The temperature results, however, are identical. Both show the same temperature (33.2^{o}C) within the ring.

8.3 Appendix C

Table 5: Number of nodes and node dimensions

Entity	Node dimension	Total Nodes
Ring	4x5	20
Skin	2x30	60
Flesh	8x30	240
Bone	7x30	210

For Q = 6900W/m3 and 7100W/m3, the ring temperature is 32.73^{o}C and 33.68^{o}C respectively.

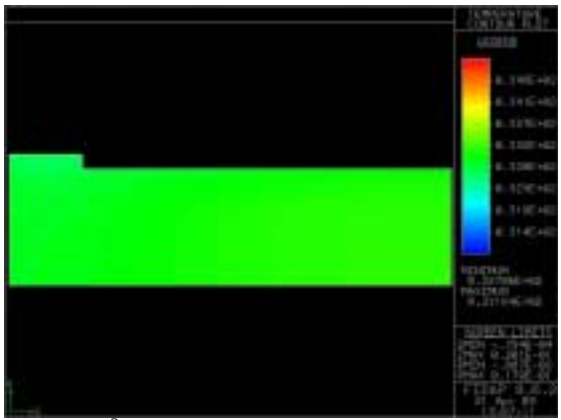

6900W/m^3 solid color plot

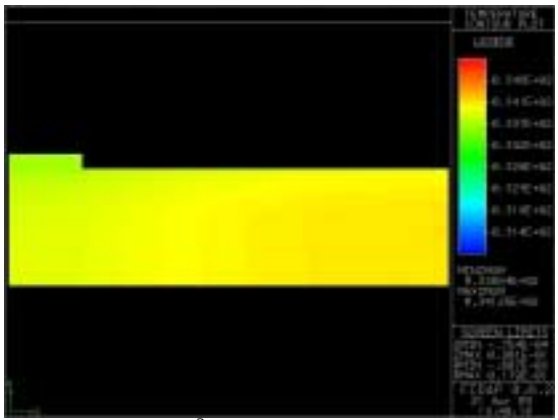

7100 W/m^3 solid color plot

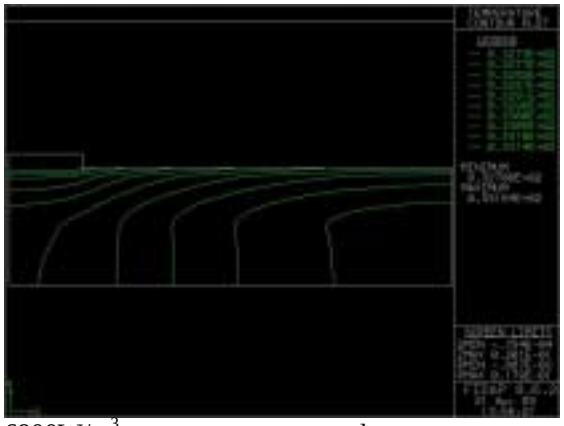

6900W/m^3 temperature contour plot

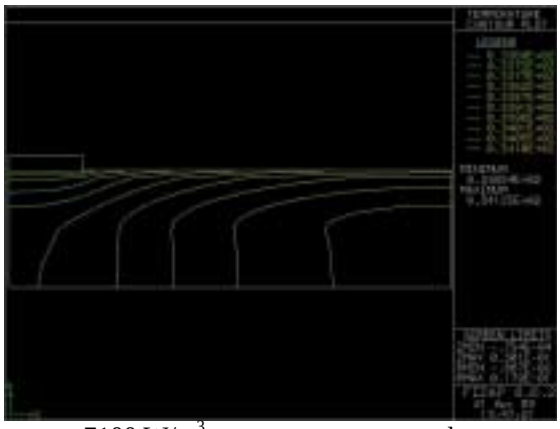

7100 W/m^3 temperature contour plot

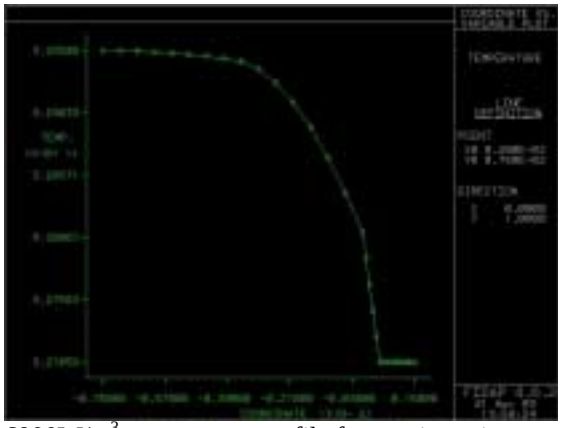

6900W/m^3 temperature profile from axis to ring

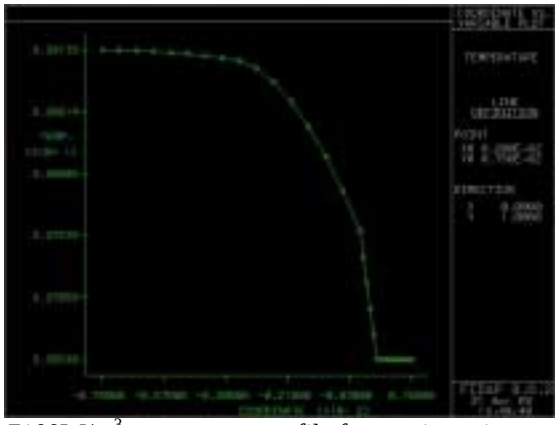

7100W/m^3 temperature profile from axis to ring

Sensitivity analysis plot: Fat layer

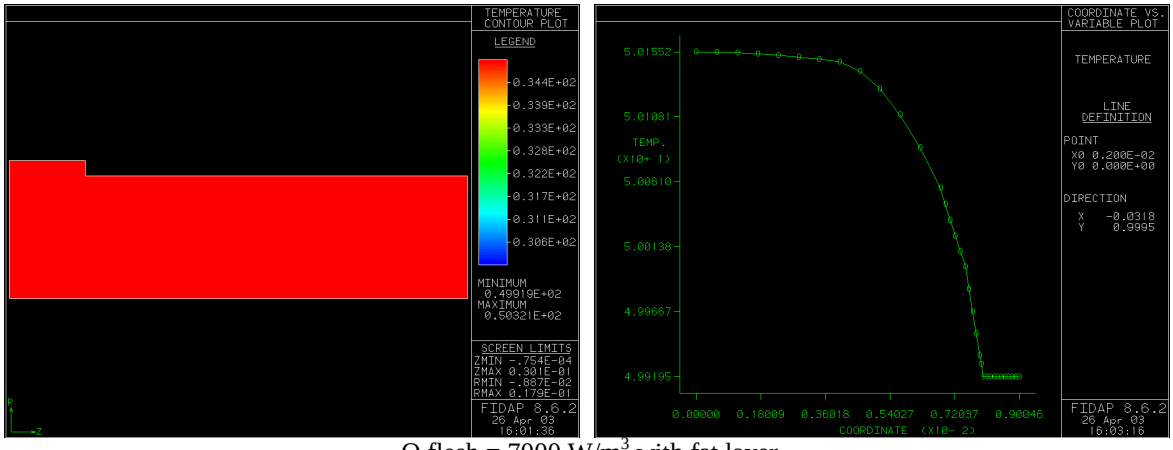

Q flesh = 7000 W/m^3 with fat layer

Sensitivity analysis plot: Bone and flesh heat generation

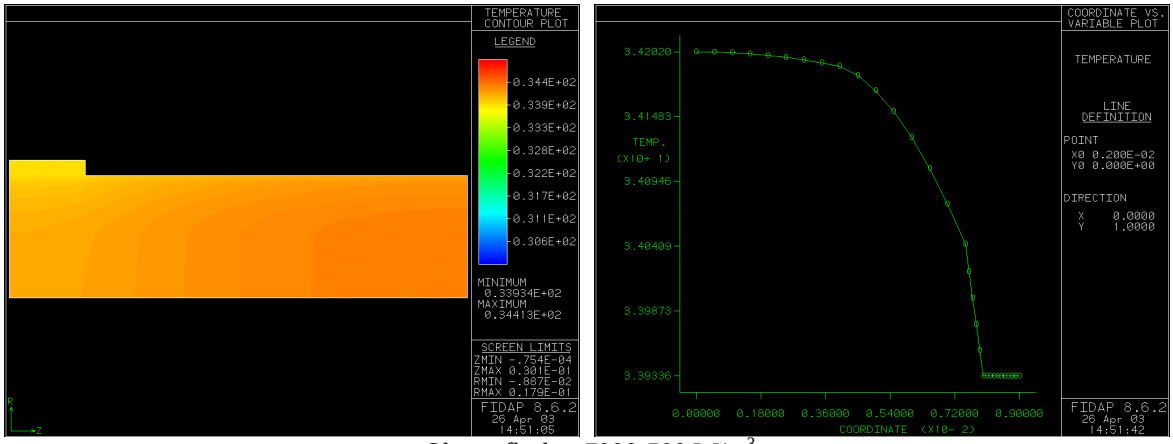

Qbone-flesh = 7000-500 W/m^3

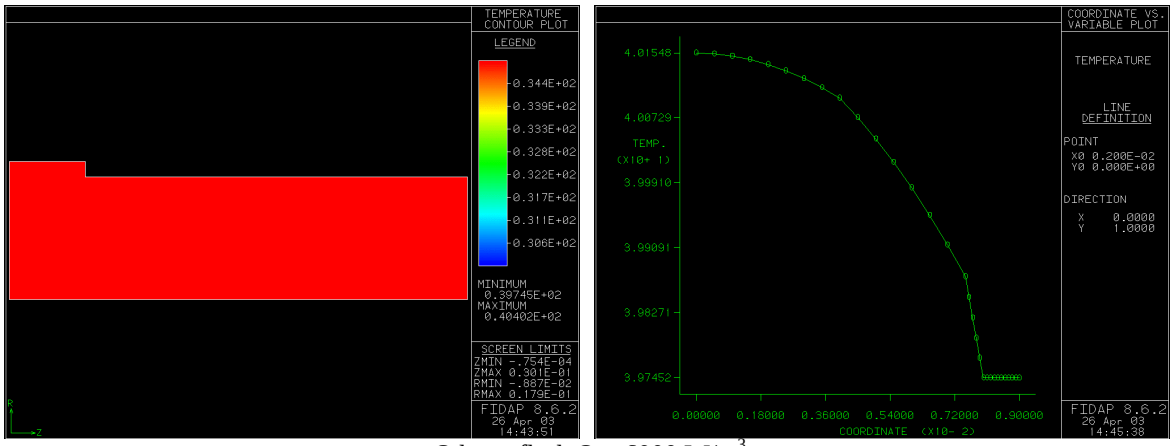

Q bone flesh Q = 6000 W/m^3

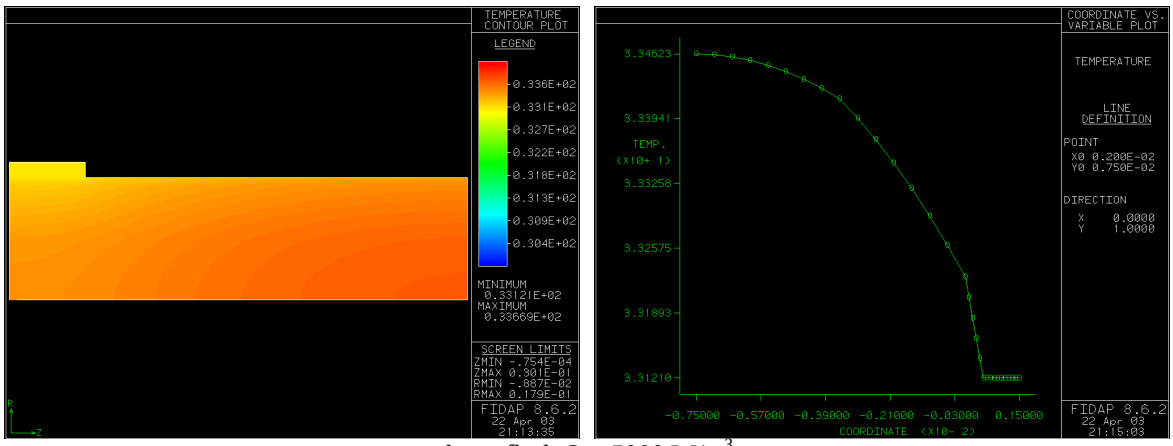

bone flesh Q = 5000 W/m^3

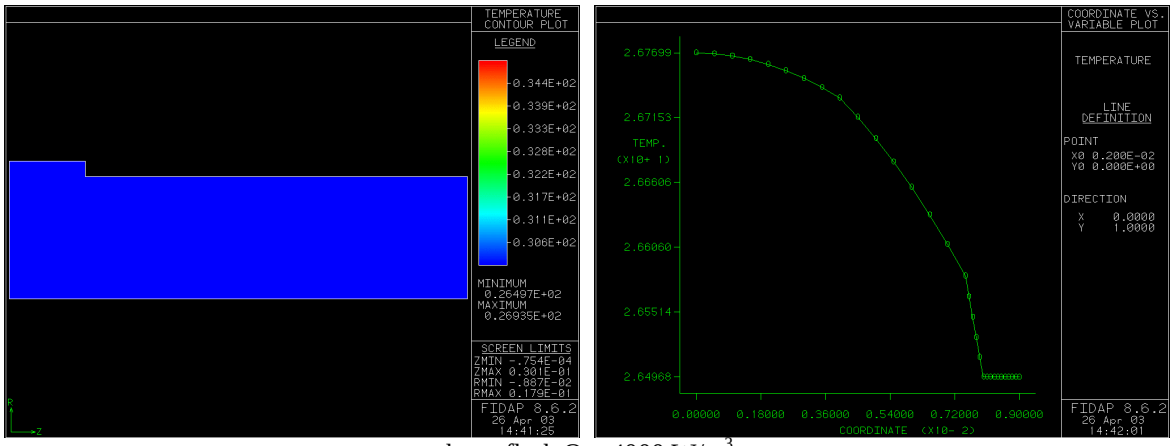

bone flesh Q = 4000 W/m^3

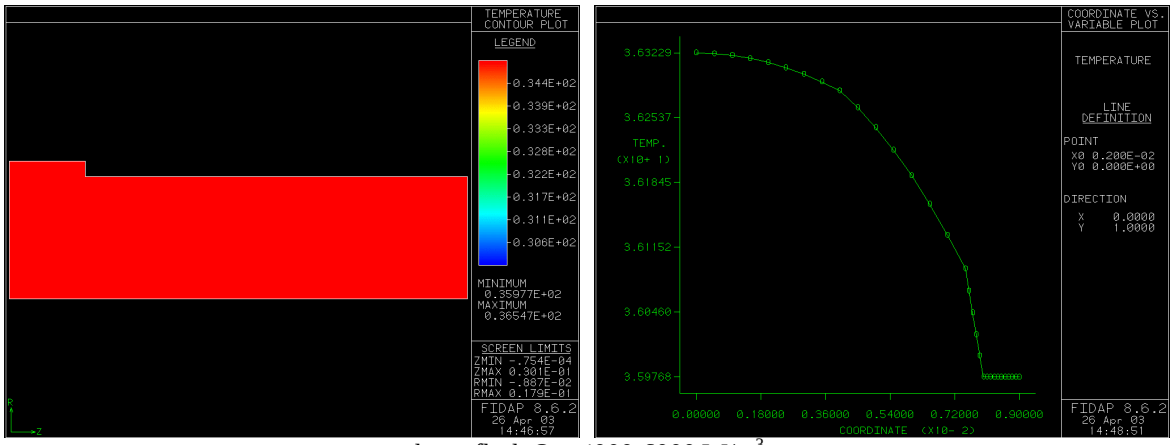

bone flesh Q = 4000-6000 W/m^3

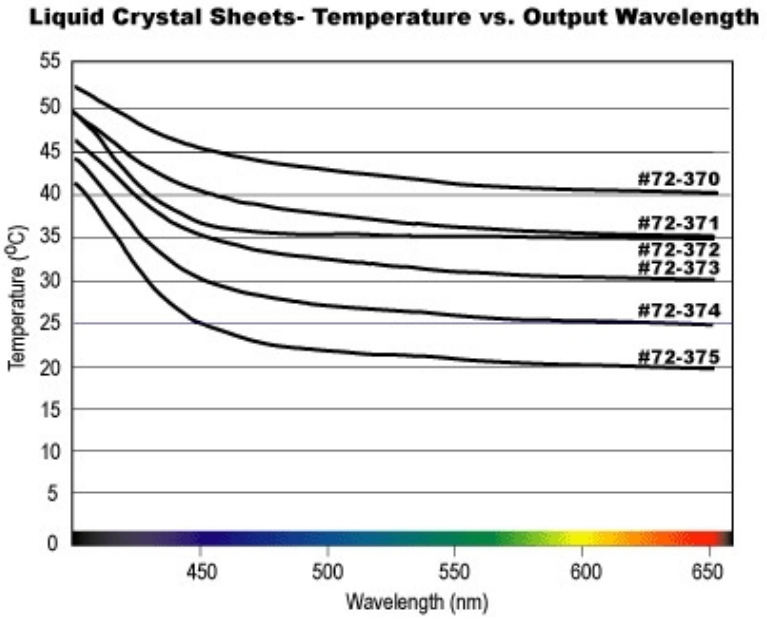

7.4 Appendix D: References

1. Chanler-Berat, D., Eckhardt, B., Reed, K., Morehead, J., Colosi, L., "Development of Frostbite in the Fingers" BEE453 Spring 2002**.**

2. Datta, K. A., Biological and Bioenvironmental Heat and Mass Transfer, Marcel Dekker, Inc: 2002. pg 112

3. Edmund Industrial Optics http://www.edmundoptics.com/IOD/DisplayProduct.cfm? productid=1642

4. Fat density: http://www.physics.carleton.ca/courses/75.502/slides/projects/1997/nkizilla

5. Fat specific heat: http://www.me.umn.edu/divisions/tht/bhmt/1_DSC_Cryomicro.pdf

6. Information on mood ring: http://home.howstuffworks.com/question443.htm

7. Other Input parameters: http://hyperphysics.phy-astr.gsu.edu/hbase/tables/thrcn.html

8. Silver properties: http://www.wikipedia.org/wiki/Silver

9. http://musr.physics.ubc.ca/~jess/sci1/biol/gradients/node1.html